Monte Carlo Perturbation Method For Optimum Surface Geometry Due To Sloshing Motion

Toshihiro Yamamoto[a*], Hiroki Sakamoto[b]

[a]*Institute for Integrated Radiation and Nuclear Science, Kyoto University, 2 Asashiro Nishi, Kumatori-cho, Sennan-gun, Osaka, 590–0494, Japan*
[b]*Independent researcher, Radiation Dose Analysis and Evaluation Network, 4–13–14, Kokubunji-shi, Tokyo, 185–0001, Japan*

Abstract

For the nuclear criticality safety of a fuel solution, it is important to identify the maximum positive reactivity induced by the upper surface sloshing motion. Deterministic methods for obtaining optimum surface geometry have been previously developed. This study proposes a Monte Carlo perturbation method for this purpose. Surface importance (*SI*) is defined as a small reactivity added by an upward lifting of a point on the upper surface. The reactivity is obtained using the correlated sampling method. The optimum geometry is attained by iteratively changing the surface geometry such that the SI distribution is eventually flattened throughout the upper surface. Examples of optimum surface geometries are presented for the bare and water-reflected fuel solutions.

Keywords: Monte Carlo; sloshing; fuel solution; criticality; perturbation

1. Introduction

Nuclear criticality safety must be ensured during all types of fissile material operation under normal and credible abnormal conditions. If the criticality safety of the fuel solution contained in a vessel is controlled by the fuel solution height, the upper surface deformation may lead to an increase in k_{eff}. Deformation is usually induced by an external force such as a seismic force. As it is difficult to identify the surface geometry during the sloshing motion of the fuel, the most conservative option in terms of nuclear criticality safety is to identify the optimum surface geometry that maximizes the k_{eff} of the fuel.

* Corresponding author
E-mail address: yamamoto.toshihiro.8u@kyoto-u.ac.jp (T. Yamamoto)

In some nuclear critical assemblies, such as the static experiment critical facility (STACY) (Yamamoto et al., 2002) and tank-type critical assembly (TCA) (Tsuruta et al., 1978), the reactivity is controlled by the height of the fuel solution or moderator. For such a critical assembly, the reactivity induced by sloshing motion is more problematic because the critical assembly is operated in a critical or slightly supercritical state. The sloshing motion may cause prompt criticality before an emergency shutdown. The development of a method for identifying the optimum surface geometry is desirable to ensure the criticality safety of fissile materials or the safe operation of critical assemblies.

Previous studies (Yamamoto and Basoglu, 1995; Yamamoto 1996) for obtaining an optimum surface geometry have already been performed based on boundary perturbation theory (Larsen and Pomraning, 1981; Rahnema, 1984). The boundary importance (BI) was defined using forward and adjoint fluxes on the outer boundary. The optimal surface geometry can be attained by iteratively changing the surface geometry so that the BI distribution eventually becomes flat on the surface. Previous studies by Yamamoto and Basoglu (1995) and Yamamoto (1996), were based on diffusion theory and transport theory, respectively, and they both used two-dimensional deterministic solvers. Meanwhile, the Monte Carlo method, which is a standard solver for nuclear criticality safety analyses, has not yet been applied to obtain optimum surface geometry. The advantage of introducing the Monte Carlo method is its flexibility in geometry description. The flexibility of the Monte Carlo method makes it suitable for searching for an optimal surface geometry because it generally has a three-dimensional shape. The objective of this study is to demonstrate the applicability of the Monte Carlo method for this purpose.

The remainder of this paper is structured as follows. In Section 2, the fundamental concept of an optimal surface geometry is revisited, and a Monte Carlo method for optimal surface geometry is proposed. In Section 3, applications of the proposed method are described. Finally, Section 4 presents the conclusions of the study.

2. Method for optimum surface geometry

2.1 Surface importance

Optimum fuel concentration distribution of a fuel solution is attained by flattening the “fuel

importance" distribution throughout the entire fuel region (Van Dam and De Leege, 1987; Hirano et al., 1991; Greenspan et al., 1999). Fuel importance is defined as the reactivity added by an infinitesimal increase in the fuel concentration at a certain position. If the fuel importance distribution is not flattened, moving some fuel from a position of lower fuel importance to a position of higher fuel importance, leaving the total amount of fuel unchanged, causes the reactivity to increase. Repeating this procedure several times eventually results in a uniform fuel importance distribution while the reactivity continues to increase. The reactivity of the fuel solution, where the fuel importance is completely uniform, does not increase further by changing the fuel concentration distribution, which implies that the reactivity is maximized.

The optimum surface geometry of a fuel solution can be determined by analogy with the optimum fuel concentration distribution. In this study, we deal with a limited situation in which a fuel solution is contained in a vessel, and only the upper surface of the fuel solution can be deformed. Similar to fuel importance, surface importance (*SI*) is defined as the reactivity caused by an infinitesimal addition of fuel at a position on the surface. The relative surface importance distribution ($SI(\boldsymbol{r}_s)$) was derived from first-order boundary perturbation theory (Larsen and Pomraning, 1981; Yamamoto 1996):

$$SI(\boldsymbol{r}_s) = \int dE \int_{\boldsymbol{n}\cdot\boldsymbol{\Omega}<0} d\boldsymbol{\Omega}\, \psi(\boldsymbol{r}_s, E, \boldsymbol{\Omega})$$

$$\times \int dE' \int_{\boldsymbol{n}\cdot\boldsymbol{\Omega}'>0} d\boldsymbol{\Omega}' \left(\Sigma_s(\boldsymbol{r}_s, E' \to E, \boldsymbol{\Omega}' \to \boldsymbol{\Omega}) + \frac{\chi(E)}{4\pi k_{eff}} \nu\Sigma_{\mathrm{f}}(\boldsymbol{r}_s, E') \right) \phi(\boldsymbol{r}_s, E', \boldsymbol{\Omega}'), \quad (1)$$

where $\boldsymbol{r}_s$ is the position vector on the outer surface, E is the energy, $\boldsymbol{\Omega}$ is the direction, $\boldsymbol{n}$ is the outer unit vector normal to the surface, ψ is the adjoint neutron flux, ϕ is the forward neutron flux, Σ_s is the scattering cross-section, $\chi(E)$ is the fission spectrum, and $\nu\Sigma_{\mathrm{f}}$ is the production cross-section. Based on Eq. (1), *SI* can be easily calculated if a neutron transport calculation code that can handle an arbitrary geometry is available, as presented in (Yamamoto, 1996).

2.2 Monte Carlo method for surface importance

If the continuous energy Monte Carlo method is used for calculating *SI*, it is not

straightforward to perform because of the difficulty in calculating the adjoint neutron flux. Recently, Monte Carlo methods have been developed to calculate the sensitivities of k_{eff} to system dimensions or reactivity caused by geometry changes (Burke and Kiedrowski, 2018; Yamamoto and Sakamoto, 2018; Li et al., 2019; Shi et al., 2020; Yamamoto and Sakamoto, 2021a). The methodologies for geometry changes in previous studies can be utilized for this study. In this study, we chose the correlated sampling method (CS) for calculating *SI*. CS has already been applied to perturbation calculations of geometry changes in fixed-source problems and *k*-eigenvalue problems (Yamamoto and Sakamoto, 2018; Yamamoto and Sakamoto, 2021a; Yamamoto and Sakamoto, 2021b).

The upper surface geometry was approximated using a polyhedron, as shown in Fig. 1, to calculate the optimum surface geometry. If a fuel solution is contained in a cylindrical vessel, the surface is approximated by a polyhedron composed of side surfaces of concentric horizontally truncated cones, owing to the symmetry of the optimum surface with respect to the central axis of the cylinder. The method proposed in this study is not limited to azimuthally symmetric geometries, but can be applied to any type of geometry that can be handled by the Monte Carlo code. Furthermore, the method can be applied to a concave geometry (reentrant surface) as far as the Monte Carlo code can handle it. As shown in (Yamamoto and Sakamoto, 2021), CS can provide an accurate reactivity caused by an interface displacement. Hence, the proposed method is capable of obtaining an optimum interface geometry as well as an optimum external outer surface geometry.

The *SI* was estimated at every vertex on the upper surface (red dots in Fig. 1). The *SI* at a vertex is approximated by the reactivity caused by a geometry perturbation, where the vertex is slightly lifted vertically upward, as shown in Fig. 2. The volume increase caused by the geometry perturbation must be constant for all vertices. Therefore, the increase in the vertex vertical position is determined such that the volume increase due to the geometry change becomes constant at every vertex. The accuracy involved in being approximated by a polyhedron can be enhanced with an increase in the number of vertices and a decrease in the volume change for the geometry perturbation.

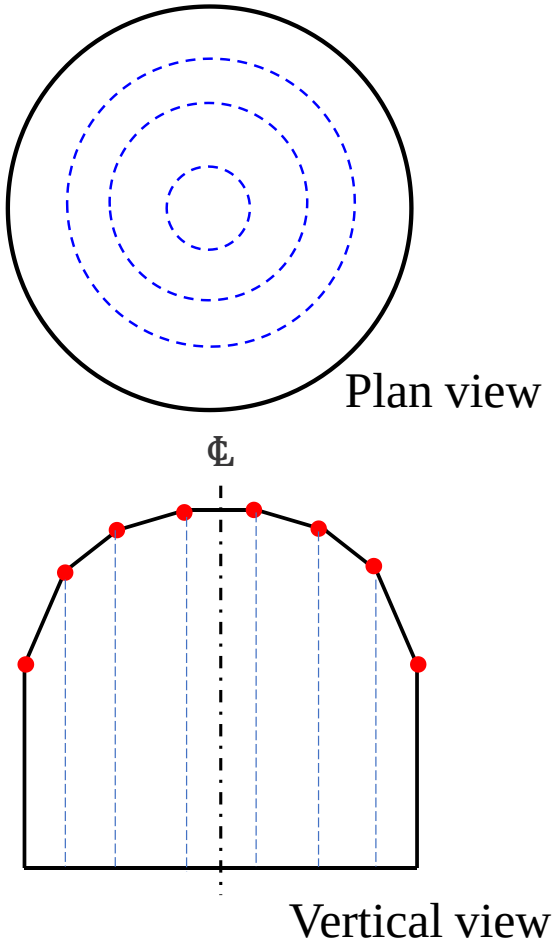

Fig. 1 Approximated cylindrical geometry composed of concentric cones

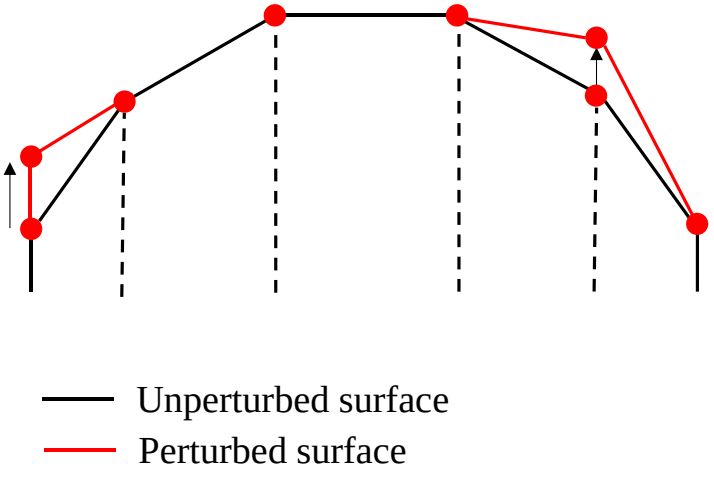

Fig. 2 Geometry perturbation for surface importance calculation

2.3 Correlated sampling method for geometry change

According to previous studies (Yamamoto and Sakamoto, 2018; 2021b), CS can provide an accurate reactivity caused by a geometry perturbation that is sufficiently small to suppress the

unbounded variance that occurs in CS for a large perturbation (Rief, 1986). Unlike other Monte Carlo perturbation methods, CS can be easily implemented. In CS, two histories (unperturbed and perturbed histories) are tracked simultaneously. The perturbed history is forced to follow the unperturbed history along the same tracks in phase space. When the two histories cross the surface that faces the perturbed geometry, the unperturbed history is terminated at the surface, whereas the perturbed history is tracked beyond the surface. A comparison between the unperturbed and perturbed histories is presented in Fig. 3. The reactivity due to geometry perturbation is caused by the perturbed history that leaves the unperturbed history behind. Therefore, the wider the unperturbed surface facing the perturbed geometry, the better the statistics of the Monte Carlo calculation. However, the perturbed geometry should be limited to some extent because a larger perturbed geometry would deteriorate the representativeness of the locality for the *SI*. If the collision estimator is used for *k*-eigenvalue calculation, the change in k_{eff} in one cycle is calculated as:

$$\Delta k_{eff}^{NP} = \frac{1}{N}\sum_{i}(w_{i,p} - w_{i,u})\frac{\nu\Sigma_f}{\Sigma_t}, \tag{2}$$

where $w_{i,p}$ and $w_{i,u}$ are the particle weights of the perturbed and unperturbed histories at the *i*th collision in the cycle, respectively. The summation is carried out at every collision in the cycle. *N* is the sum of the starting particle's weight in the cycle. Because $w_{i,p}$ is equal to $w_{i,u}$ until the unperturbed history terminates at the surface facing the perturbed geometry, Eq. (2) is expressed equivalently as follows:

$$\Delta k_{eff}^{NP} = \frac{1}{N}\sum_{i>i_p} w_{i,p}\frac{\nu\Sigma_f}{\Sigma_t}, \tag{3}$$

where i_p denotes the last collision of the unperturbed history before termination, as shown in Fig. 3.

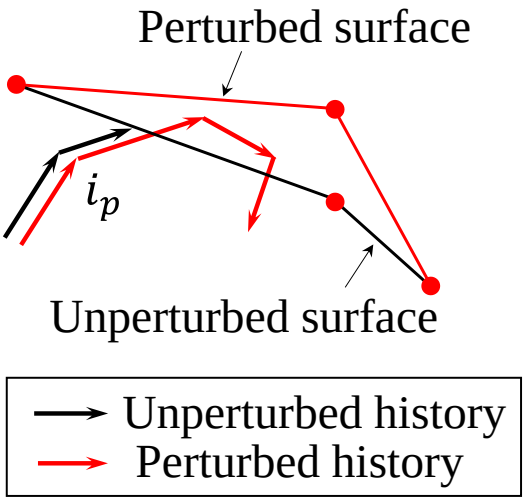

Fig. 3 Unperturbed and perturbed histories in correlated sampling method

This geometric change leads to a perturbation in the fission source distribution. Eq. (2) does not account for fission source perturbation. Similar to many other Monte Carlo perturbation methods, perturbation of the fission source distribution needs to be considered (Nakagawa and Asaoka, 1978; Nagaya and Mori, 2011; Griesheimer and Goter, 2015; Kim et al., 2018; Griesheimer and Gibson, 2019; Tuya and Nagaya, 2022). This study adopted the method developed by Nagaya and Mori (2005) for fission source perturbations. In this method, the perturbed fission source effect is propagated from one cycle to the next until the effect converges to the equilibrium state. At each fission source site, the ratio of the fission source weight of the perturbed history to the weight of the unperturbed history is assigned to the fission source that is used for the next cycle calculation. In the next cycle, the ratio is updated at the fission source site and the new ratio is assigned to the progeny of the fission source in the previous cycle. This propagation cycle for fission source perturbation is repeated until the ratio fully converges. Ten propagation cycles are known to be adequate. The algorithm for fission source perturbation estimation is involved and it is omitted in this paper. For more details on the algorithm, refer to (Nagaya and Mori, 2005).

The Monte Carlo calculation with the CS perturbation calculation can be performed only once for all vertices where the *SI* needs to be estimated. However, a relatively high data storage capacity is required to estimate the fission source perturbation effect. The amount of data to be stored is the

product of the number of histories per cycle, the number of propagation cycles (approximately ten cycles), and the number of vertices. Monte Carlo algorithms such as the Wielandt method and the superhistory method would be available to reduce the memory consumption at the expense of increased computation time (Choi and Shim, 2016; Yamamoto, 2018; Shi et al., 2020).

2.4 Convergence towards optimum surface geometry

This section presents a method for obtaining an optimum surface geometry using an *SI* distribution calculated using the CS. An example of optimum surface geometry is shown here for a fuel solution contained in a cylindrical vessel. We started with an upright cylindrical geometry with a horizontally flat upper surface. The entire geometry of the fuel solution was divided into a cylinder (for the innermost region) and several concentric annuli, as shown in Fig. 4. Owing to the symmetry of the cylindrical geometry, it was assumed that the upper surface of the innermost cylinder was always horizontally flat even in the optimum surface geometry. Geometry perturbations to the innermost and outermost vertices are added, as shown in Figs. 5 and 6, respectively. A perturbation to the remaining vertex was added, as shown in Fig. 7. As stated in Section 2.2, the volume increase caused by the geometry perturbation must be constant for every vertex. The reactivity of the perturbation to each vertex was calculated using the CS. Using the reactivity at each vertex, the new vertical position of the vertex for the next calculation is determined as follows:

$$h_i' = h_i + C\left(SI_i - \overline{SI_i}\right), \tag{4}$$

where h_i and h_i' are the vertical positions at the *i*th vertex before and after the iteration, respectively; C is an arbitrary positive constant; SI_i is *SI* at the *i*th vertex; $\overline{SI_i}$ is the arithmetic mean of SI_i. The operation by Eq. (4) lifts vertices whose *SI* are higher than the average, whereas it depresses vertices whose *SI* are smaller than the average. Because the volume of the fuel solution determined by h_i' deviates from the initial volume, h_i' is adjusted such that the volume is conserved after the iteration, as follows:

$$h_i'' = h_i' \cdot \frac{V_0}{V'}, \tag{5}$$

where V_0 is the initial volume of the fuel solution, V' is the volume determined by h_i', h_i'' is

the adjusted volume to be used for the next iteration.

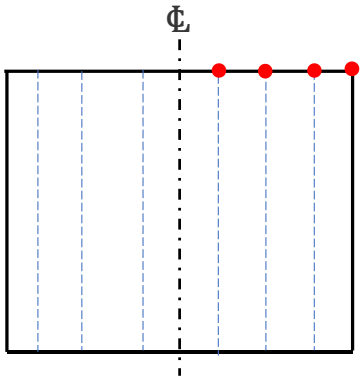

Fig. 4 Initial state of fuel solution for optimum geometry

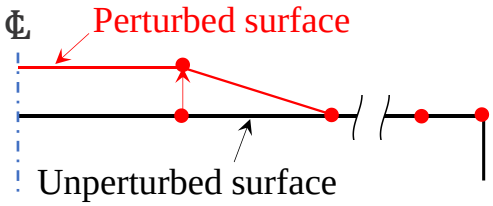

Fig. 5 Perturbation to the innermost vertex

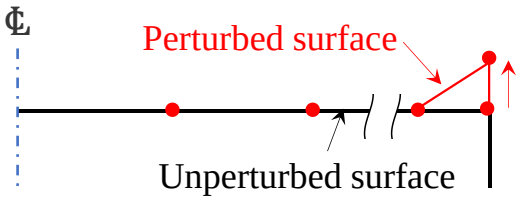

Fig. 6 Perturbation to the outermost vertex

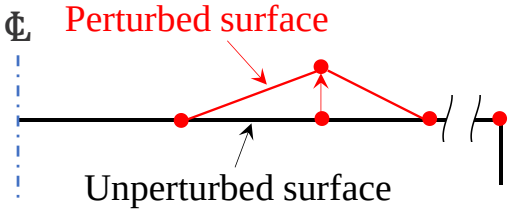

Fig. 7 Perturbation to the remaining vertices

This procedure was repeated until the *SI* distribution was sufficiently flat. As an index of the flatness of the *SI*, the convergence index is defined as follows:

$$CI = \sqrt{\sum_{i=1}^{N} \left(\frac{SI_i}{\overline{SI_i}} - 1 \right)^2} \quad , \tag{6}$$

where N denotes the total number of vertices. This iteration was repeated until CI fell below a certain value.

In summary, the optimum surface geometry is obtained by the following procedure.

(1) Set up vertices on the outer surface of the initial geometry.

(2) Calulate SI_i for the ith vertex by slightly lifting the vertical position of the vertex. This calculation is performed individually for every vertex on the surface.

(3) After SI_i is obtained for all vertices, the vertical position of each vertex is updated according to Eq. (4).

(4) Using Eq. (5), the vertical position of each vertex is adjusted in order to conserve the volume of the fuel solution.

(5) Repeat steps (2) through (4) until the convergence index CI, defined by Eq. (6), is below a prescribed value.

The optimum surface geometry of the fuel solution in a cylindrical vessel is typically illustrated in Fig. 8 (Yamamoto and Basoglu, 1995). However, if a fuel solution has a horizontally long shape, the SI cannot be flattened, even if the height of the outermost vertex is zero, as shown in Fig. 9(a). The optimum geometry of such a shallow fuel solution eventually converges towards a spherical geometry, as shown in Fig. 9(b). However, the Monte Carlo code that the authors developed for this study is not designed to converge to a sphere as the optimum geometry. If one of h_i's becomes below zero, the code terminates the iteration process. To achieve convergence to a sphere as the optimum geometry, it is necessary to program a Monte Carlo code with that consideration. This study focuses on a situation in which an optimum surface geometry is given, as shown in Fig. 8, and a shallow fuel solution, where the optimum geometry is ultimately given by spherical geometry, is excluded.

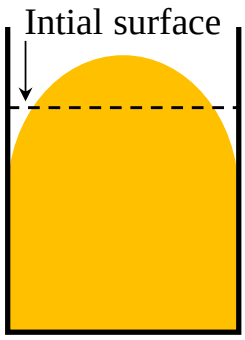

Fig. 8 Typical optimum geometry of bare cylindrical fuel solution

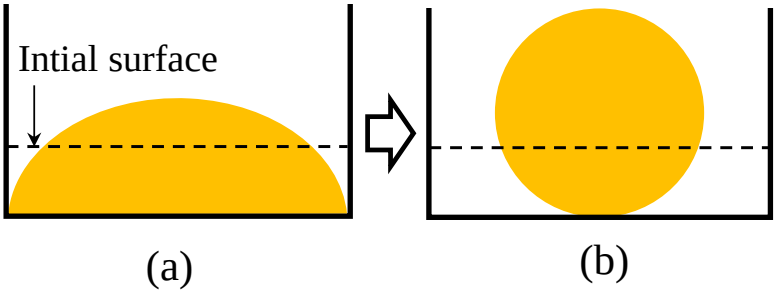

Fig. 9 Optimum geometry of shallow fuel solution

3. Optimum surface geometry of cylindrical fuel solution

3.1 Verification of correlated sampling method

Before presenting an example of optimum surface geometry, the verification of the CS method is presented for geometry perturbation. All calculations in this study were performed using a cylindrical geometry. The fuel was 9.97 wt.%-enriched uranyl nitrate solution. The uranium concentration was 253.6 g/L, and the acidity was 2.24 mol/L. The calculations were performed using an in-house multigroup Monte Carlo solver. Three energy group constants for the fuel solution were prepared using the SRAC code system (Okumura et al., 2007). Anisotropic scattering was considered up to the P_1 order. The group constants of the fuel solution are presented in Table 1. The verification calculations were performed for the geometry shown in Fig. 10.

Table 1 Three-group constants of solution fuel

	1st group (10 MeV~235 keV)	2nd group (235 keV~0.993 eV)	3rd group (0.993 eV~)
Σ_t (cm^{-1})	2.8799E-1*	1.19352	2.48124
Σ_c (cm^{-1})	5.6022E-4	5.9008E-3	2.4670E-2
$\nu\Sigma_f$ (cm^{-1})	6.6739E-4	2.5205E-3	6.9313E-2
χ fission spectrum	0.957934	0.042066	—
$\Sigma_{s0g\to g}$ (cm^{-1})**	2.0206E-1	1.1058	2.4277
$\Sigma_{s1g\to g}$ (cm^{-1}) ***	1.5785E-1	6.9876E-1	9.5817E-1
$\Sigma_{s0g\to g+1}$ (cm^{-1}) **	8.5095E-2	8.0729E-2	—
$\Sigma_{s1g\to g+1}$ (cm^{-1}) ***	2.7175E-2	2.9489E-2	—

*Read as 2.8799×10^{-1}, **P_0 component, ***P_1 component

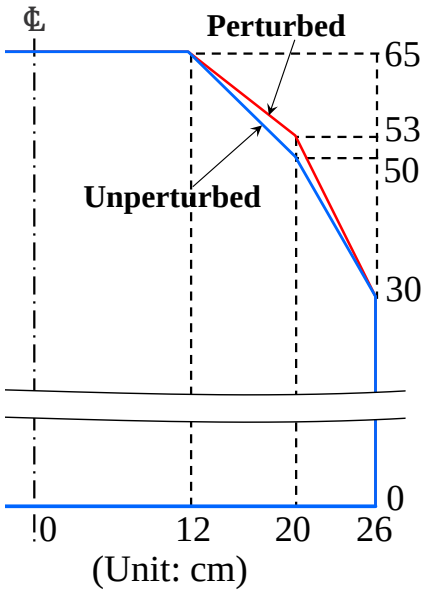

Fig. 10 Perturbed and unperturbed geometries for verification calculation

The reference solution was obtained using the difference in k_{eff} between two independent Monte Carlo calculations for the perturbed and unperturbed geometries. The calculations were performed with 200,000 histories per cycle, 30 inactive cycles, and 8,000 active cycles. The number of propagation cycles for fission source perturbation was 12. The results of the CS agreed with the reference within the statistical uncertainties, as shown in Table 2. In this numerical example, the fission source perturbation effect was relatively large, which accounted for more than half of the k_{eff} change without fission source perturbation.

Table 2 k_{eff} changes due to the surface perturbation for verification

Correlated sampling method (pcm)	Δk_{eff}^{NP} [b]	1051.4 ± 0.4[a]
	Δk_{eff}^{PS} [c]	−709.4 ± 0.6
	Total	342.0 ± 0.8
Reference (pcm)		341.9 ± 2.0

[a] One standard deviation

[b] Δk_{eff}^{NP}: k_{eff} change without fission source perturbation

[c] Δk_{eff}^{PS}: k_{eff} change due to fission source perturbation

3.2 Optimum surface geometry of bare fuel solution

The optimum surface geometry was obtained for a bare fuel solution with cylindrical geometry, as shown in Fig. 11. The diameter was 56 cm, and the initial height of the solution was 62 cm. Although the solution was assumed to be contained in an upright cylindrical vessel, the vessel wall was not included in the calculation model. The geometry was divided into eight regions. The radii of the regions were 2.5, 5.0, 8.0, 12.0, 16.0, 20.0, 23.0, and 26.0 cm. The initial k_{eff} was 0.91079 ± 0.00001.

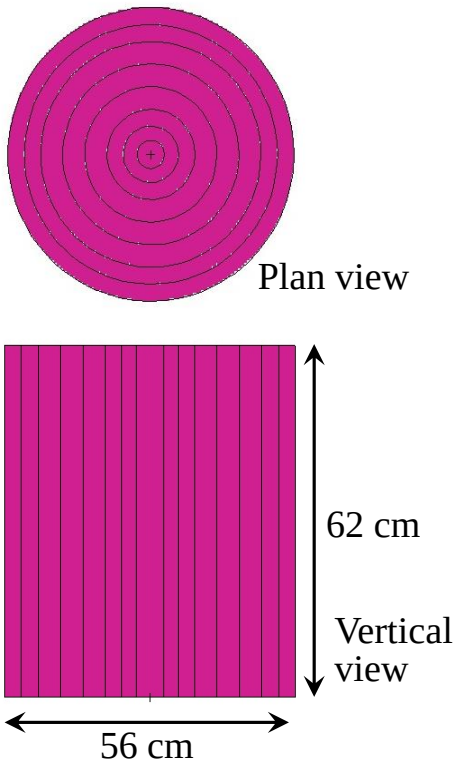

Fig. 11 Initial geometry of bare fuel solution

The perturbation to the innermost vertex was added by vertically lifting the vertex between the innermost cylinder and adjacent annulus by 0.5 cm, as shown in Fig. 5. The increase in the height at the remaining vertices was determined such that the volume change due to the perturbation was the same as that of the innermost perturbation. All perturbation calculations using the CS method were performed with 200,000 histories per cycle, 30 inactive cycles, and 6,000 active cycles.

The Monte Carlo calculations for the optimum surface geometry were repeated eight times until the convergence index *CI*, defined by Eq. (6), was less than 0.1. The arbitrary constant, *C*, in Eq. (4) was 200,000. The *SI* distributions of the initial state, 1st, 2nd, and 7th (final) iterations are shown in Fig. 12. The error bar for one standard deviation is smaller than the symbol size. The final geometry of the fuel solution is illustrated in Fig. 13. The increase in k_{eff} from the initial state versus the iteration number is shown in Fig. 14. The *CI* versus the iteration number is shown in Fig. 15. As shown in Figs. 14 and 15, k_{eff} reasonably increases with a decrease in *CI*, indicating that k_{eff} increases as the *SI* becomes flatter.

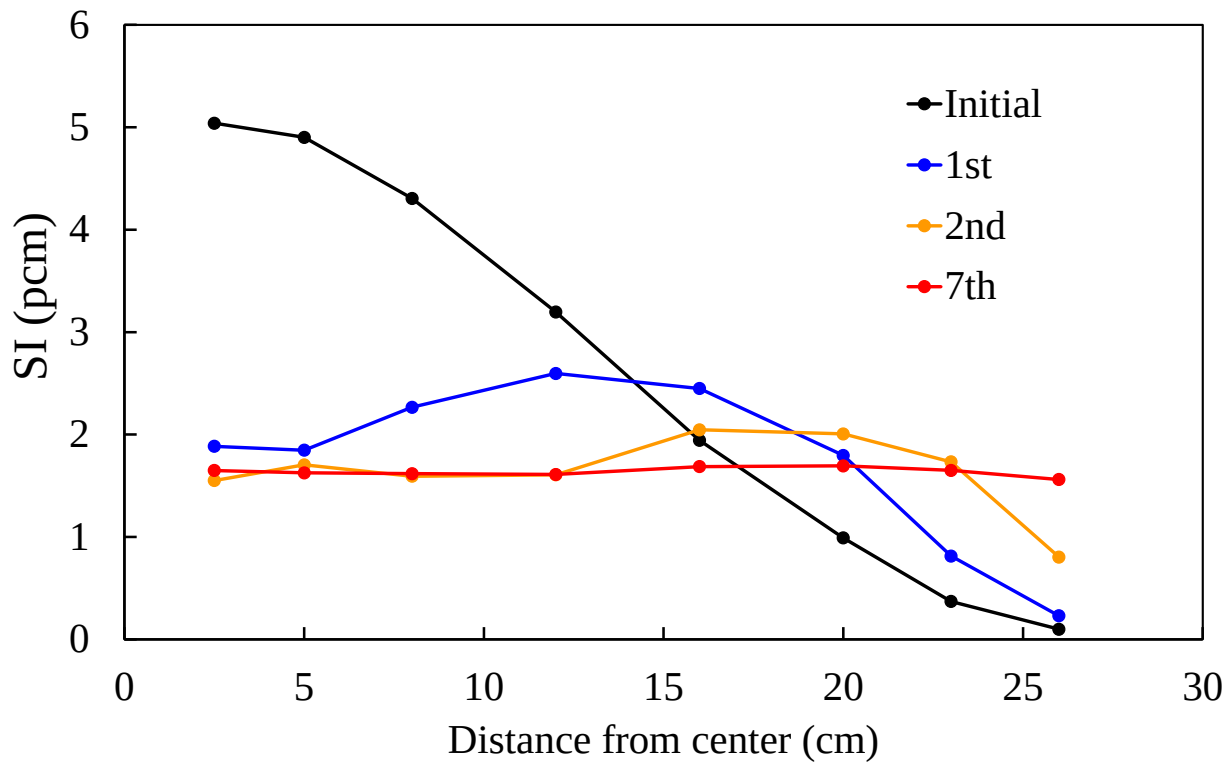

Fig. 12 Surface importance distribution of bare fuel solution

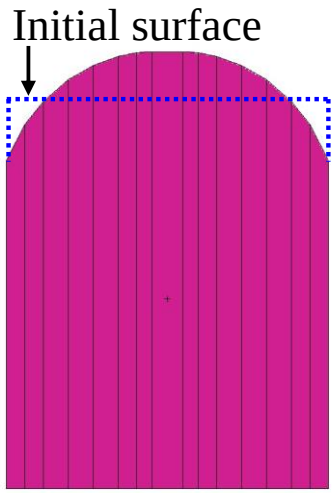

Fig. 13 Final geometry of bare fuel solution after 7th iteration

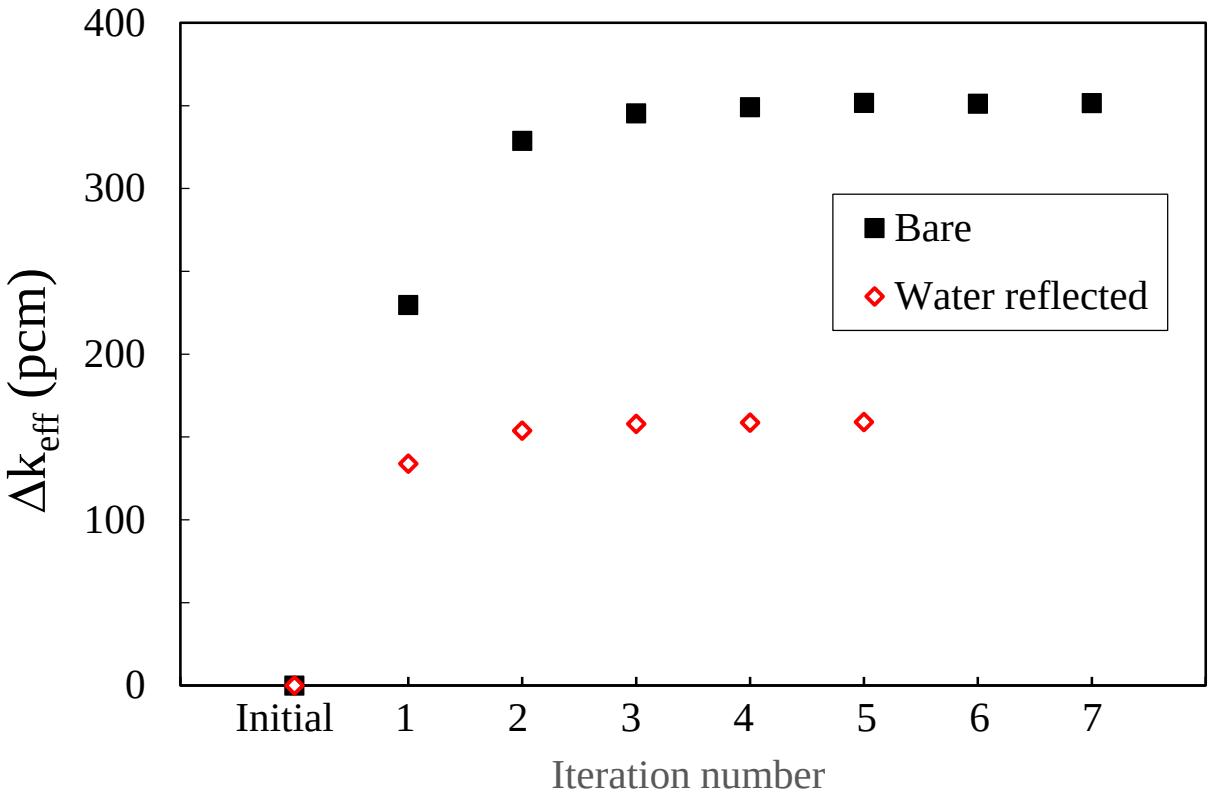

Fig. 14 Increase of k_{eff} versus iteration number

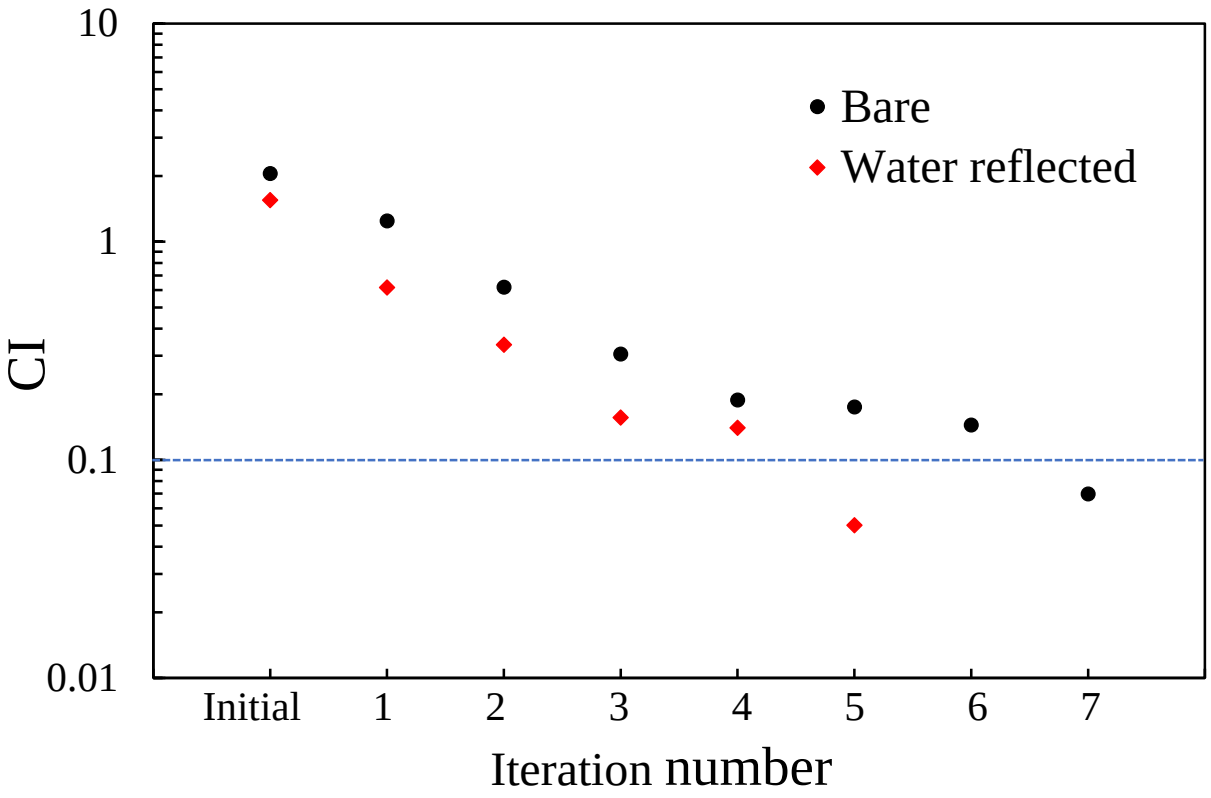

Fig. 15 Convergence index versus iteration number

3.3 Optimum surface geometry of water reflected fuel solution

The optimum surface geometry was obtained for a light water-reflected fuel solution, as shown in Fig. 16. The material, geometry, and calculation conditions were the same as those described in Section 3.2, except that the side surface of the fuel solution was surrounded by a 5 cm-thick light water reflector. The group constants of light water are listed in Table 3. The initial k_{eff} was 0.95134 ± 0.00001.

Table 3 Three-group constants of light water reflector

	1st group (10 MeV~235 keV)	2nd group (235 keV~0.993 eV)	3rd group (0.993 eV~)
Σ_t (cm^{-1})	2.9767E-1*	1.3054	2.5605
Σ_c (cm^{-1})	2.8640E-4	4.3300E-4	1.6150E-2
$\Sigma_{s0g\to g}$ (cm^{-1})**	2.1000E-1	1.2222E+0	2.5444E+0
$\Sigma_{s1g\to g}$ (cm^{-1}) ***	1.4952E-1	7.7311E-1	8.6888E-1
$\Sigma_{s0g\to g+1}$ (cm^{-1}) **	8.7358E-2	8.2727E-2	—
$\Sigma_{s1g\to g+1}$ (cm^{-1}) ***	3.4803E-2	3.5369E-2	—

*Read as 2.9767×10^{-1}, **P_0 component, ***P_1 component

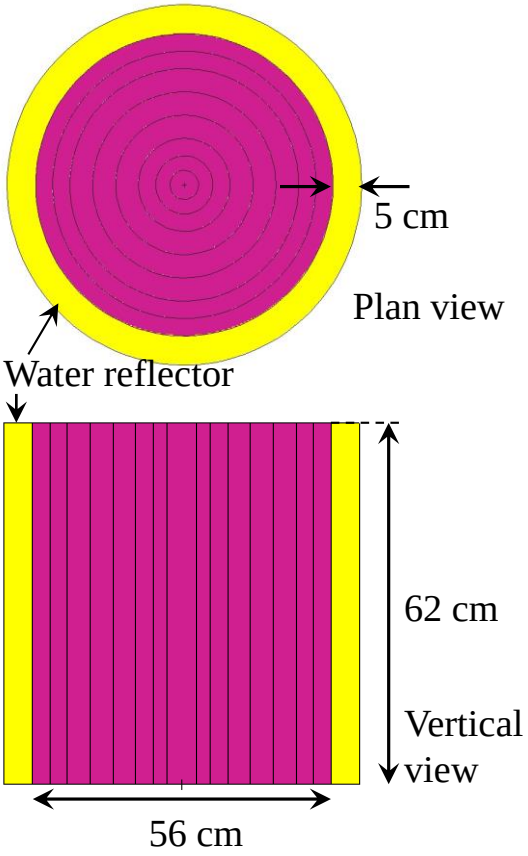

Fig. 16 Initial geometry of water-reflected fuel solution

While the *SI* decreases from the center to the outer surface in a bare fuel, as shown in Fig. 12, the *SI* in a water-reflected fuel does not simply decrease owing to the effect of the reflector. It is anticipated that the initial *SI* distribution and optimum surface geometry are more moderate in water-reflected fuel than in bare fuel.

Monte Carlo calculations for the optimum surface geometry were repeated six times until the *CI* was less than 0.1. The arbitrary constant, *C*, in Eq. (4) was 150,000. The *SI* distributions of the initial state, 1st, 2nd, and 5th (final) iterations are shown in Fig. 17. The *SI* of the initial state at the interface between the fuel and reflector was larger than that at 23 cm from the center. The final geometry of the fuel solution is shown in Fig. 18. As expected, the final surface geometry was flatter than that of the bare fuel solution. The increase in k_{eff} from the initial state versus the iteration number is shown in Fig. 14. The *CI* versus the iteration number is shown in Fig. 15. The increase in k_{eff} induced by the optimum surface geometry was less than half of that of the bare

solution fuel.

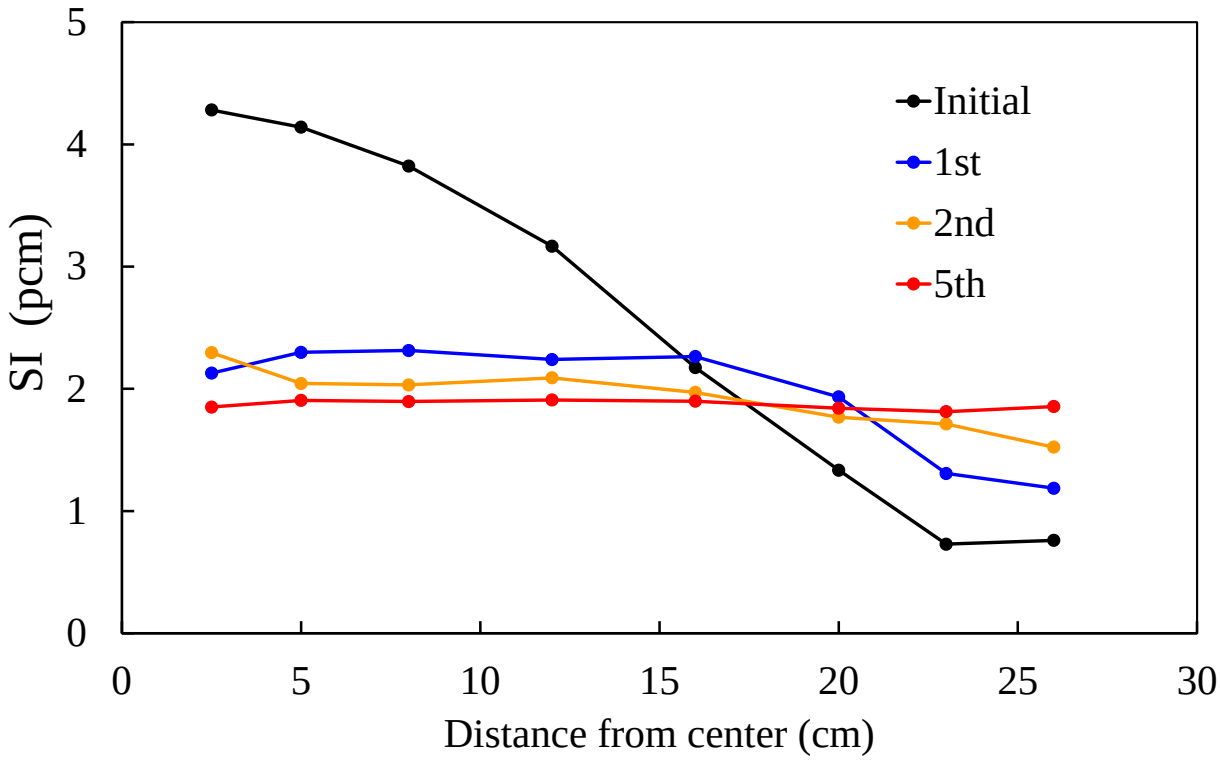

Fig. 17 Surface importance distribution of water reflected fuel solution

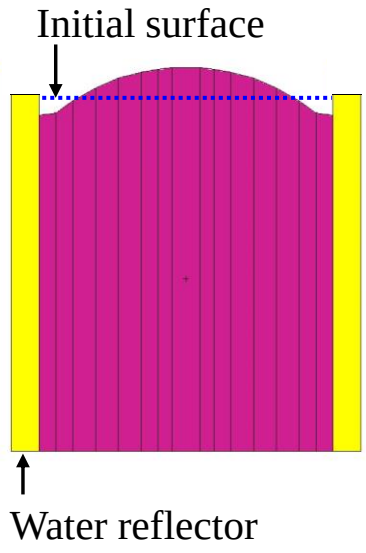

Fig. 18 Final geometry of water reflected fuel solution after 5th iteration

4. Conclusions

Deterministic methods for obtaining the optimum surface geometry of a fuel solution have already been developed based on neutron diffusion or transport theory by the author of this paper.

This study presents a new Monte Carlo method for obtaining optimum surface geometry. Optimum surface geometry is attained by flattening surface importance (*SI*) distribution on the entire surface to be deformed. *SI* is defined as the reactivity caused by an infinitesimal addition of fuel at a position on the surface. To calculate *SI* using the Monte Carlo method, *SI* is approximated by the reactivity caused by a slight lift of a slight portion of the surface. This study adopted the correlated sampling method (CS) to calculate *SI*. The *SI* is expressed by the change in k_{eff} caused by geometric perturbation. After the *SI* distribution is calculated on the surface, the surface geometry is updated by lifting the surface position with a higher *SI* and depressing the surface position of the lower *SI* while preserving the volume of the fuel solution. This procedure is iterated until the *SI* is sufficiently uniform over the entire surface. In the examples of this study, the number of iterations was less than ten.

The example in this study dealt with a cylindrical geometry, which is a substantially two-dimensional problem. Therefore, the number of data points where the *SI* needs to be calculated is very limited. The number of data points becomes much greater for a three-dimensional problem, such as a fuel solution in a rectangular vessel. However, as stated in Section 2.3, the Monte Carlo calculation for one iteration can be performed only once if a relatively large data storage capacity is available for perturbation propagation.

The CS method proposed in the study is not an exact one because *SI* is approximated by the small reactivity caused by the small change of surface height. The application of an exact Monte Carlo perturbation method for the sensitivity of the surface displacement will be the subject of future work. One of the potential candidates will be the development of the differential operator sampling method that provides the reactivity derivative with respect to changes in surface height.

References

Burke, T.P., Kiedrowski, B.C., 2018. Monte Carlo perturbation theory estimates of sensitivities to system dimensions. Nucl. Sci. Eng. 189, 199–223. https://doi.org/10.1080/00295639.2017.1388093.

Choi, S.H., Shim, H.J., 2016. Memory-efficient calculations of adjoint-weighted tallies by the Monte Carlo Wielandt method. Ann. Nucl. Energy 96, 287-294.

https://dx.doi.org/10.1016/j.anucene.2016.06.011.

Greenspan, E., Karni, Y., Petrie, L.M., Regev, D., 1999. SWANS: a prototype SCALE criticality sequence for automated optimization using SWAN methodology. ORNL/TM-1999/274.

Griesheimer, D.P., Gibson, N.A., 2019. Simplified method for estimating the effective delayed neutron fraction with Monte Carlo correlated sampling. Proc. Int. Conf. Mathematics and Computational Methods Applied to Nuclear Science and Engineering (M& C2019), Portland, Oregon, August 25–29, 2019.

Griesheimer, D.P., Goter, T.P., 2015. Estimating the effective neutron generation time with Monte Carlo correlated sampling. Proc. Int. Conf. Mathematics and Computations, Supercomputing in Nuclear Applications and Monte Carlo, (M & C+SNA+MC 2015), Nashville, Tennessee, April 19–23, 2015.

Hirano, Y., Yamane, Y., Nishina, K., 1991. Reactivity effect of non-uniformly distributed fuel in fuel solution systems. J. Nucl. Sci. Technol. 28, 595–607. https://doi.org/10.3327/jnst.28.595.

Kim, S.H., Yamanaka, M., Pyeon, C.H., 2018. Improvement of fission source distribution by correlated sampling method in Monte Carlo perturbation calculations. J. Nucl. Sci. Technol. 55, 945–954. https://doi.org/10.1080/00223131.2018.1452649.

Larsen, E.W., Pomraning, G.C., 1981. Boundary perturbation theory. Nucl. Eng. Sci. 77, 415–425. https://doi.org/10.13182/NSE81-A18954.

Li, H., Yu, G., Huang, S., Zhou, M., Shi, G., Wang, K., 2019. Calculating the k-eigenvalue sensitivity to typical geometric perturbations with the adjoint weighted method in the continuous-energy reactor Monte Carlo code RMC. Nucl. Sci. Eng. 193, 1186–1218. https://doi.org/10.1080/00295639.2019.1614800.

Nagaya, Y., Mori, T., 2005. Impact of perturbed fission source on the effective multiplication factor in Monte Carlo perturbation calculations. J. Nucl. Sci. Technol. 2, 428–448. https://dx.doi.org/10.3327/jnst.42.428.

Nagaya, Y., Mori, T., 2011. Estimation of sample reactivity worth with differential operator sampling method. Prog. Nucl. Sci. Technol. 2, 842–850. https://dx.doi.org/10.15669/pnst.2.842.

Nakagawa, M., Asaoka, T., Improvement of correlated sampling Monte Carlo methods for reactivity calculations. J. Nucl. Sci. Technol., 15, 400–410. https://doi.org/10.3327/jnst.15.400.

Okumura, K., Kugo, T., Kaneno K, Tsuchihashi, K., 2007. SRAC2006: A comprehensive neutronics calculation code system. JAEA-Data/Code 2007-004.

Rahnema, F., 1984. Internal interface perturbations in neutron transport theory. Nucl. Sci. Eng. 86, 76–90. https://doi.org/10.13182/NSE84-A17971.

Rief, H., 1984. Generalized Monte Carlo perturbation algorithms for correlated sampling and a second-order Taylor series approach. Ann. Nucl. Energy 9, 455–476. https://doi.org/10.1016/0306-4549(84)90064-1.

Shi, G, Yu, G., Jia, C., Wang, K., Huang, S., Cheng, Q., Li, H., 2020. Superhistory-based differential operator method for generalized responses sensitivity calculations. Ann. Nucl. Energy 140, 107291. https://doi.org/10.1016/j.anucene.2019.107291.

Shi, G., Feng, Z., Conglong, J., Wang, K., Huang, S., Cheng, Q., 2020. Geometric sensitivity analysis of generalized response function with RMC code. Ann. Nucl. Energy 149, 107824. https://doi.org/10.1016/j.anucene.2020.107824.

Tsuruta, H., Kobayashi, I., Suzaki, T., Ohno, A., Murakami, K., Matsuura, S., 1978. Critical sizes of light-water moderated UO_2 and PuO_2-UO_2 lattices. Japan Atomic Energy Research Institute, JAERI-1254.

Tuya, D., Nagaya, Y., 2022. Adjoint-weighted correlated sampling for *k*-eigenvalue perturbation in Monte Carlo calculation. Ann. Nucl. Energy 169, 108919. https://doi.org/10.1016/j.anucene.2021.108919.

Van Dam, H., De Leege, P.F.A., 1987. Minimum critical mass system. Ann. Nucl. Energy 14, 369–376. https://doi.org/10.1016/0306-4549(87)90116-2.

Yamamoto, T., Basoglu, B., 1995. Optimal geometry for fuel solution sloshing based on the boundary perturbation theory. Ann. Nucl. Energy 22, 649–658. https://doi.org/10.1016/0306-4549(94)00096-W.

Yamamoto, T., 1996. Most critical geometry of a fuel solution based on the transport boundary

perturbation theory. J. Nucl. Sci. Technol. 33, 78–82. https://dx.doi.org/10.3327/jnst.33.78.

Yamamoto, T., Miyoshi, Y., Kikuchi, T., Watanabe, S., 2002. Criticality safety benchmark experiment on 10% enriched uranyl nitrate solution using 28 cm-thickness slab core. J. Nucl. Sci. Technol. 39, 789–799.

Yamamoto, T., 2018. Eigenvalue sensitivity analysis capabilities with the differential operator method in the superhistory Monte Carlo method. Ann. Nucl. Energy 112, 150-157. https://dx.doi.org/10.1016/j.anucene.2017.10.002.

Yamamoto, T., Sakamoto, H., 2018. Monte Carlo perturbation methods using ‘‘virtual density” theory for calculating reactivity due to geometry change. Ann. Nucl. Energy 119, 362–373. https://doi.org/10.1016/j.anucene.2018.05.006.

Yamamoto, T., Sakamoto, H., 2021a. Monte Carlo perturbation calculation for geometry change in fixed source problems with the perturbation source method. Prog. Nucl. Energy 132, 103611. https://doi.org/10.1016/j.pnucene.2020.103611

Yamamoto, T., Sakamoto, H., 2021b. Exact Monte Carlo calculation method for *K*-eigenvalue change using perturbation source method. J. Nucl. Sci. Technol. 58, 886–898.

List of figures

Declaration of competing interest

The authors declare that they have no known competing financial interests or personal relationships that could have appeared to influence the work reported in this paper.